VIETNAM NATIONAL UNIVERSITY, HANOI
UNIVERSITY OF ENGINEERING AND TECHNOLOGY

LƯU VIỆT HƯNG

OPERATIONAL DETECTION AND MANAGEMENT OF SHIPS IN VIETNAM COASTAL REGION USING VNREDSAT-1 IMAGE

MASTER THESIS IN COMPUTER SCIENCE

HANOI – 2016

VIETNAM NATIONAL UNIVERSITY, HANOI
UNIVERSITY OF ENGINEERING AND TECHNOLOGY

LƯU VIỆT HƯNG

OPERATIONAL DETECTION AND MANAGEMENT OF SHIPS IN VIETNAM COASTAL REGION USING VNREDSAT-1 IMAGE

Major: Information Technology

Sub-Major: Computer Science

Mã số: 60480101

MASTER THESIS IN COMPUTER SCIENCE

ADVISOR: DR. NGUYEN THI NHAT THANH

HANOI – 2016

STATEMENT ON ACADEMIC INTEGRITY

I hereby declare and confirm with my signature that the thesis is exclusively the result of my own autonomous work based on my research and literature published, which is seen in the notes and bibliography used. I also declare that no part of the thesis submitted has been made in an inappropriate way, whether by plagiarizing or infringing on any third person's copyright. Finally, I declare that no part of the thesis submitted has been used for any other paper in another higher education institution, research institution or educational institution.

Hanoi, 28/10/2016

Student

Luu Viet Hung

ACKNOWLEDGEMENT

Firstly I would like to express my respect and my special thanks to my supervisor Dr. Nguyen Thi Nhat Thanh, VNU University of Engineering and Technology, for the enthusiastic guidance, warm encouragement and useful research experiment.

Secondly, I greatly appreciate my supervisor Dr. Bui Quang Hung and co-worker in Center of Multidisciplinary Integrated Technologies for Field Monitoring, VNU University of Engineering and Technology, for their encouragements and insightful comments.

Thirdly, I am grateful to all the lecturers of VNU University of Engineering and Technology, for their invaluable knowledge which they taught to me during academic years.

Last but not least, my family is really the biggest motivation behind me. My parents, my brother, my sister-in-law and my little nephew always encourage me when I have stress and difficulties. I would like to send them my gratefulness and love.

The work done in this thesis was supported by Space Technology Institute, Vietnam Academy of Science under Grant VT-UD.06/16-20.

TABLE OF CONTENT

LIST OF TABLES

LIST OF FIGURES

ABSTRACT

Recent years have witness the new trend of developing satellite-based ships detection and management method. In this thesis, we introduce the potential ship detection and management method, which to the best of our knowledge, is the first one made for Vietnamese coastal region using high resolution pan images from VNREDSat-1. Operational experiments in two coastal regions including Saigon River and South China Sea with different conditions show that the performance of proposed ship detection is promising with average accuracies and recall of 92.4% and 93.2%, respectively. Furthermore, the ship detection method is robustness to different sea-surface and cloud cover conditions thus can be applied to new satellite image domain and new region.

Chapter 1 INTRODUCTION

1.1 Motivation

Recently, marine ship monitoring in coastal region is an increasingly important task. Due to the lack of in-time information, many coastal regions around the world have been facing threats from uncontrolled activities of ship. To improve our ability to manage coastal areas with sustainability in mind, there is in need for real time tools capable of detecting and monitoring the marine ship activities.

Traditionally, marine management in coastal region relied mainly on the exchanging data between an automatic tracking system on-board of ships and vessel traffic services (VTS) with other nearby ships or in-land base stations. The International Maritime Organization's International Convention for the Safety of Life at Sea requires Automatic Identification System (AIS) to be fitted aboard international voyaging ships with gross tonnage of 300 or more, and all passenger ships regardless of size. While AIS was originally designed for short-range operation, the long-range identification and tracking (LRIT) of ships was also established as an international system from May 2016. However, in order to obtain AIS and LRIT data, the coastal region manager depend their work to the willing participation of the vessel involved.

From the manager perspective, here a question arises “How could we quickly response to extreme events in case the vessel refuse to cooperate or in rescues operations when on-board system like LRIT and AIS not available?” It is common scenarios for managing ships involved in illegal activities on the waters, e.g. as illegal fishery, pollution, immigration, or ships in recuse area.

To enhance ship management in coastal region, the usage of satellite technology for ship detection and monitoring applications has been recently increasing thanks to the widely use of Synthetic Aperture Radar (SAR) and high resolution optical images. Both are proven to be very promising in detection of ship.

Synthetic aperture radar (SAR) is a form of radar that is used to create images of objects either in two or three dimensional representations. To create a SAR image, successive pulses of radio waves are transmitted to illuminate a target scene, and the echo of each pulse is received and recorded. The pulses are transmitted and the echoes received using a single beam-forming antenna, with wavelengths of a meter down to several millimeters. This characteristic helps SAR images less affected by weather conditions such as cloud, day/night scene [11-13] and can be utilized to estimate velocity of ship target [12]. Ships appear as bright objects in Synthetic Aperture Radar (SAR) images because they are strong reflectors of the radar pulses emitted by the satellite as shown in Figure 1.1. Up to date, several sources of SAR image are currently available such as Sentinel-1, ALOS-PALSAR, RADARSAT-1 and ENVISAT ASAR …

Figure 1.1. Appearance of ships in Synthetic Aperture Radar image captured by Sentinel (Source: ESA)

The main disadvantage of SAR is that their spatial resolution is limited so that it is difficult to detect a ship below 15 meters' length. Ship detection on optical satellite images can extend the SAR based systems. The main advantage of optical satellite images is that they can have very high spatial resolution, thus enabling the detection of small ships, and enhancing further ship type recognition.

In the last decades, optical satellite images have many applications in meteorology, oceanography, fishing, agriculture, biodiversity conservation, forestry, as well as many other disciplines. Images provide by optical sensor onboard can be in visible multi-spectral colors and in many other spectra. In the field. There are four types of resolution when discussing optical satellite imagery in remote sensing: spatial, spectral, temporal, and radiometric where:

- Spatial resolution: the pixel size of an image representing the size of the surface area (i.e. m^2) being measured on the ground
- Spectral resolution: is defined by the wavelength interval size and number of intervals that the sensor is measuring
- Temporal resolution: the amount of time that passes between imagery collection periods for a given surface location
- Radiometric resolution: number of levels of brightness and the effective bit-depth of the sensor (number of gray scale levels)

Generally, there are trade-off between these resolutions. Because of technical constraints, optical satellite can only offer the following relationship between spatial and spectral resolution: a high spatial resolution is associated with a low spectral resolution and vice versa. The different spatial and spectral resolutions are the limiting factor for the utilization of the satellite image data for different applications.

In the field of maritime ship detection as well as many other object recognition in optical satellite image, spatial resolution is usually lay emphasis up on as the most important resolution. Very high resolution optical imagery such as IKONOS, GEOEYE, Quickbird, Worldview, … are widely used as the input of ship detection application. These satellites provide images with up to sub-meter resolution in black and white Panchromatic (PAN) band and lower resolution multispectral images (typically Red, Green, Blue and Near Infrared). Ship detection system utilizing these data could deliver detail spatial feature information on small ship targets. Figure 1.2 shows the example of ship appearance in SPOT 5 PAN image with resolution of 2.5m.

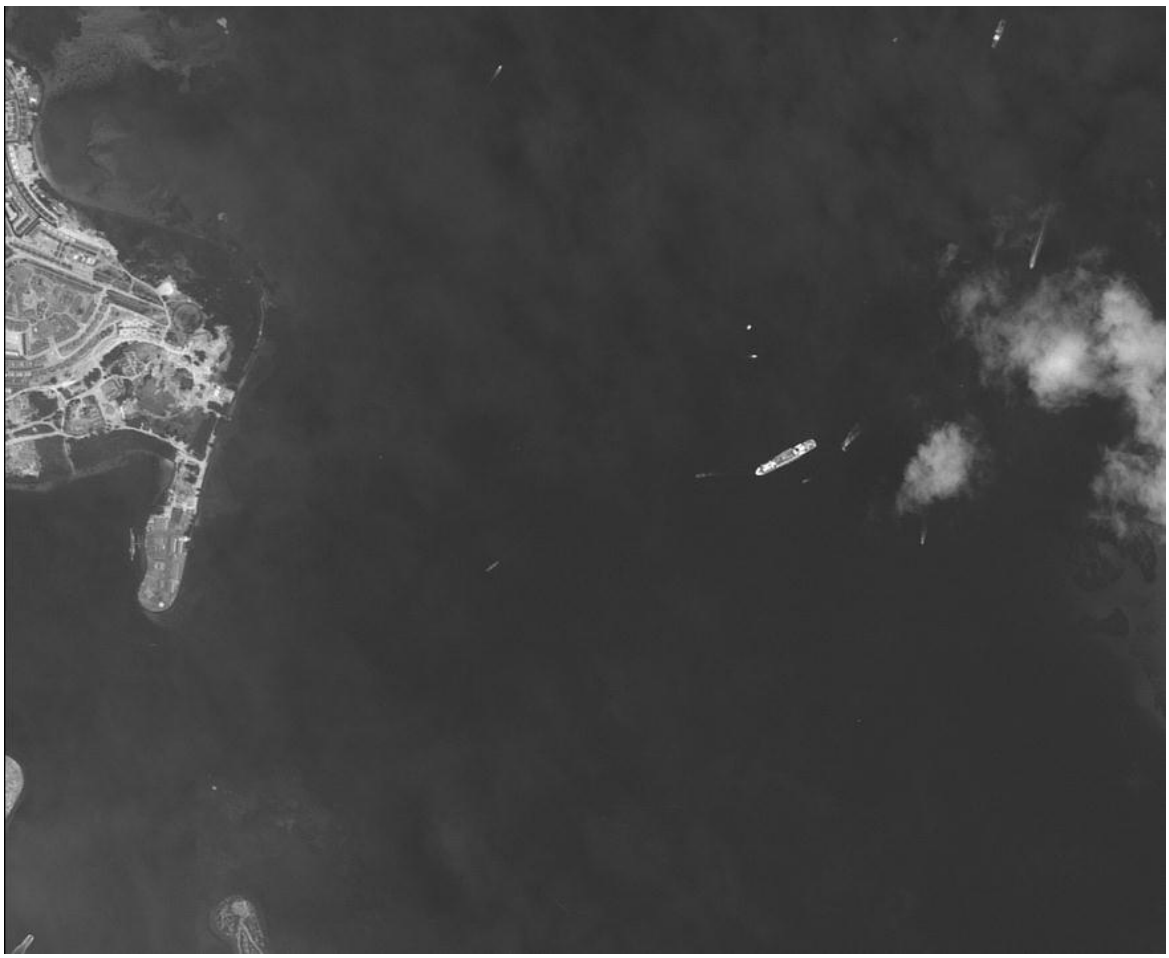

Figure 1.2. Appearance of ships in SPOT 5 PAN image (Source: Airbus Defense and Space)

The drawback of ship detection using optical satellite images is that (i) they can only work during daytime and (ii) weather and sea surface conditions heavily affect the performance of detection approach.

Since the challenge of (i) can only be solved by the system which combine optical images with SAR images to provide more frequent monitoring, researchers around the world pay most attention to tackle two challenges implied by (ii).

First, it is difficult to extract ships from complex backgrounds as represented in Figure 1.3. In natural images, the loss and false alarms in ship detection can be affected by the complex sea surface, the appearance of interference objects (e.g. cloud, waves, shore, and port) which is very similar to the ship, and the variant in both ship shape and size itself.

Second, due to the big size of optical satellite images (e.g. a VNREDSat-1 image has the size of ~9000×9000 pixels), an effective and fast method is much in demand when big data meet a platform with limited computation.

Figure 1.3. Appearance of ships in image with complex background. Strong textures sea surface and cloud can strongly affect the ship detection performance.

Launched in 2013, VNREDSat-1 (Vietnam Natural Resources, Environment and Disaster Monitoring Satellite) is the first optical Earth Observing satellite

of Vietnam. Its primary mission is to monitor and study the effects of climate change, and to predict, take measures to prevent natural disasters, and optimize the management of Vietnam's natural resource [32].

The use of VNREDSat-1 data is recently increasing in many applications focus on Vietnam region. However, how optical image especially VNREDSat-1 can be applicable for maritime ship detection and management in Vietnam coastal region is the question not yet answered. To the best of my knowledge, there is little to no existing works investigate ship detection problem in Vietnam though it is very popular worldwide. Since very high resolution optical satellite image from other source is usually very expensive and SAR coverage area in Vietnam is very limited, VNREDSat-1 image can be prominent as a cheap and widely Vietnam coverage source of data.

1.2 Objectives

Motivated by aforementioned problems, challenges as well as recent advances in space technology development, this thesis focus on developing an operational ship detection algorithm utilizing VNREDSat-1 optical imagery.

The main objectives of this thesis are threefold. First, this thesis focuses into the use of satellite imagery for ship detection to allow other researchers better understanding of the capabilities, the advantages, and drawbacks of existing approaches.

Second, it is to understand in detail the ship detection and classification procedure on optical satellite imagery.

Third, experiment results of ship detection using VNREDSat-1 images in coastal region of Vietnam are investigated. It would help drive the development of future sensors and platforms towards the operational needs of ship monitoring.

The work in this thesis is part of the national project in the framework of National Space Program.

1.3 Contributions and thesis structure

The main contributions of this thesis are twofold. First, the state-of-the-art report and literature review of ship detection and classification in optical satellite images is provided. Second, the operational ship detecting method is implemented and its results are investigated.

The rest of the thesis is organized as follows. In Chapter 2, the review of related state-of-the-art works in the field of ship detection from optical satellite image are presented. In Chapter 3, the operational method of ship detection from optical image is defined and the experiment results using VNREDSat-1 image is presented in Chapter 4. Conclusion is drawn in Chapter 5.

Chapter 2 LITERATURE REVIEW OF SHIP DETECTION USING OPTICAL SATELLITE IMAGE

The goal of this chapter is to review the state-of-the-art methods of ship detection. General speaking, all the existing ship detection approach consists of two main stages: candidate's selection and classification. This chapter is divided into two sections as followed.

In Section 2.1, the way how ship candidates extracted in different methods is analyzed with their advantages and disadvantages. The pros and cons of many innovative ship classification methods are presented in Section 2.2. Finally, the discussion of how algorithm is chosen for each stage is presented in Section 2.3.

2.1 Ship candidate selection

Existing works on ship candidates' selection can be divided into three main groups.

The first group performs pixel wise labeling to address the foreground pixels and then group them into regions by incorporating region growing approach. These methods focus on the difference in gray values between foreground object including ships and other inferences such as clouds, wake … and background sea surface. A threshold segment method is applied to produce the binary image and then post-processed using morphological operators to remove noises and connect components. This approach has a major problem. Since the lack of prior analysis on sea surface model, parameters and threshold values of these methods are usually empirical chosen, which lacks the robustness. They may either over segment the ship into small parts or make the ship candidate merge to nearby land or cloud

regions [31]. [1] was the first to develop a method for the detection of ships using the contrast between ships and background of PAN image. In [4] the idea of incorporating sea surface analysis to ship detection using PAN image was first declared. They defined two novel features to describe the intensity distribution of majority and effective pixels. The two features cannot only quickly block out no-candidate regions, but also measure the Intensity Discrimination Degree of the sea surface to assign weights for ship candidate selection function automatically. [23] re-arrange the spatially adjacent pixels into a vector, transforming the Panchromatic image into a "fake" hyper-spectral form. The hyper-spectral anomaly detection named RXD [24, 25] was applied to extract ship candidates efficiently, particularly for the sea scenes which contain large areas of smooth background.

The methods in second group incorporating bounding box labeling. [15, 26, 27] detected ships based on sliding windows in varying sizes. However, only labeling bounding boxes is not accurate enough for ship localization; thus, it is unsuited for ship classification [16]. [28, 29] detected ships by shape analysis, including ship head detection after water and land segmentation and removed false alarms by labeling rotated bounding box candidates. These methods depend heavily on detecting of V-shape ship heads which is not applicable for small-size ship detection in low resolution images (2.5m or lower).

In [16] the author proposed ship rotated bounding box which is the improvement of the second group. Ship rotated bounding box space using modified version of BING object-ness score [30] is defined which reduce the search space significant. However, this method has low Average Recall in compare to pixel-wise labeling methods.

2.2 Ship classification

Following the first stage of candidates selection, accurate detection is aim to find out real ships accurately. Several works using supervised and unsupervised classifier are investigated in this section.

In [1], based on a known knowledge of ships' characteristics, spectral, shape and textural features is screen out the ones that most probably signify ship from other objects. A set of 28 features in three categories were proposed. Such a high dimensional data set requires a large training sample while a limited amount of ground truth information is available concerning ship position. Therefore, Genetic Algorithm is used to reduce the dimension. Finally, the Neural Network was trained to accurately detect ships.

In [4], there are only two shape features are used in combination with a decision tree to eliminate false alarm. Shi et al. [23] deployed Circle Frequency (CF) and Histogram of Gradient (HOG) to describe the information of ship shape and the pattern of gray values of ships.

With the rise of deep learning, scientific researchers pay more attention on object detection by convolutional neutral networks (CNN). It can not only deal with large scale images, but also train features automatically with high efficiency. The concept of CNN was used by [29] and [16]. The advantage of CNN is that it can train features automatically with high efficiency instead of using predefined features. However, these methods required a very large high-quality dataset. Besides, to pick an optimized network topology, learning rate and other hyper-parameters is the process of trial and error.

2.3 Operational algorithm selection

In summary, various approaches have been investigated in this field. However, some open issues still exist for each method groups. The choice of which candidate selection algorithm and which specific learning algorithm should be used is a critical step. Ideally, the chosen two-stage approach should be robust to the variant of remote sensing images and be able to process the data efficiently since the image is usually large.

In the first stage of candidate selection, the method proposed by Yang et al. [4] is chosen mainly because of its linear time computation characteristic in compare with other algorithm in pixel-wise group. Despite its robustness, the methods in second and third group are not considered since they usually provide low recall of ship target extracted.

In the second stage, Convolution Neural Network is the latest advances in field of machine learning and seems to outperform other supervised classifiers. However, due to the fact that the size of data provided by VNREDSat-1 is limited up to now, CNN could not perform well since it needs a very large high-quality dataset. In this thesis, supervised techniques are considered and CNN will be considered in the future works. Chosen of a supervised technique is done by performing statistical comparisons of the accuracies of trained classifiers on specific datasets.

In the next Chapter, the operational method of ship detection using in this thesis is detailed.

Chapter 3 THE OPERATIONAL METHOD

The goal of this Chapter is to implement an operational method which robustly detects ships in various backgrounds conditions in VNREDSat-1 Panchromatic (PAN) satellite images. The framework is demonstrated in Figure 3.1.

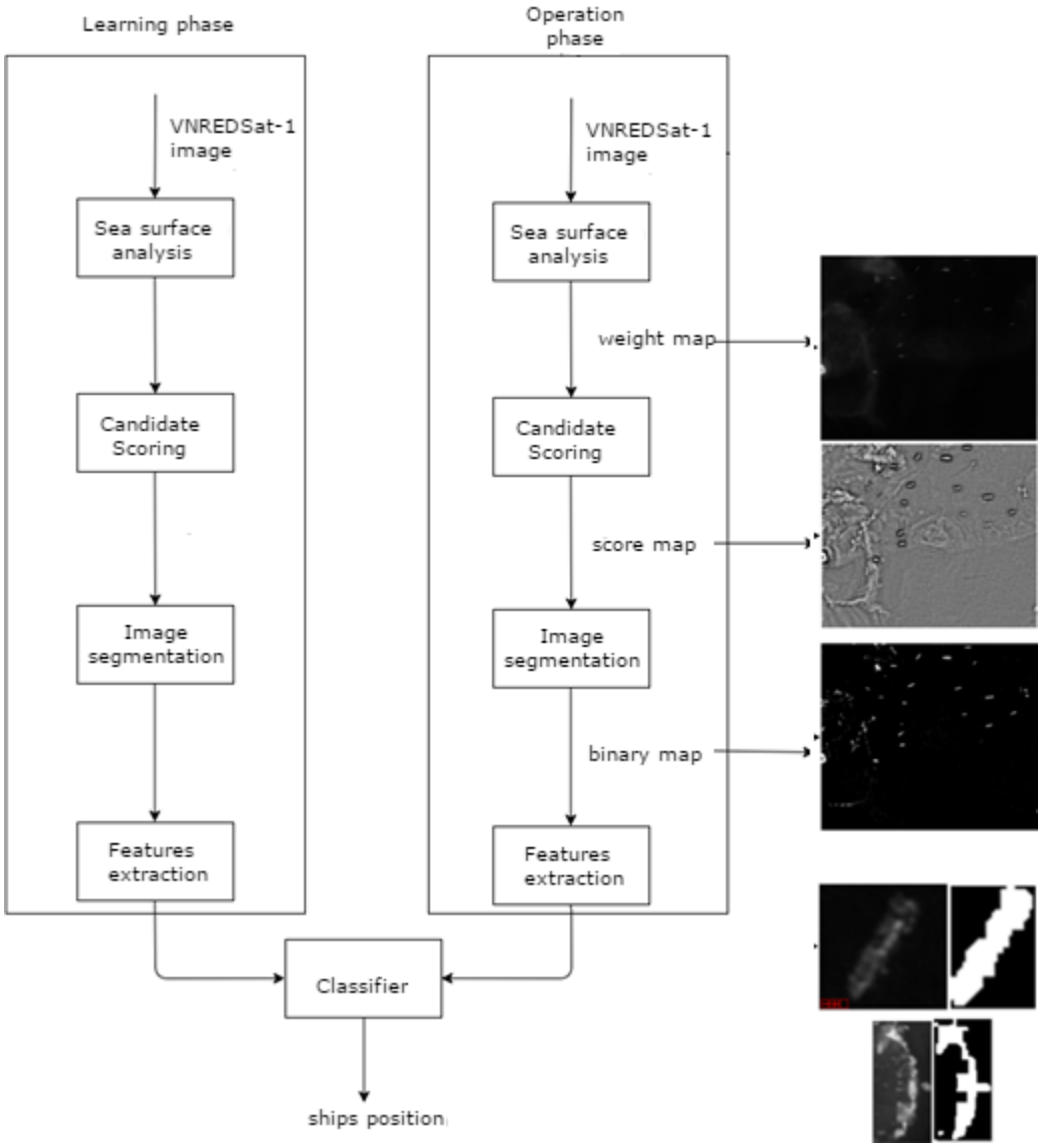

Figure 3.1 The processing flow of the proposed ship detection approach

The method consists of two main processing stages including pre-detection stage and classification stage. In the pre-detection stage, a sea surface analysis is

first applied to measure the complexity of the sea surface background. The output of this analysis is then used as the weights for the scoring function based on the anomaly detection model to extract potential ship candidates. In the latter stage, three widely-used classifiers including Support Vector Machine (SVM), Neural Network (NN) and CART decision tree (CART) are used for the classification of potential candidates.

3.1 Sea surface analysis

Sea surfaces show local intensity similarity and local texture similarity in optical images. However, ships as well as clouds and small islands, destroy the similarities of sea surfaces [4]. Hence, ships can be viewed as anomaly in open oceans and can be detected by analyzing the normal components of sea surfaces.

Sea surfaces are composed of water regions, abnormal regions, and some random noises [4]. Moreover, most of intensities of abnormal regions are different from the intensities of sea water, and the intensity frequencies of abnormal regions are much less than that of sea water. Therefore, the intensity frequencies of the majority pixels will be on the top of the descending array of the image histogram.

Three features namely Majority Intensity Number and Effective Intensity Number proposed by [4] are used to describe the image intensity distribution on the majority and the effective pixels, respectively. Intensity Discrimination Degree is concluded from these two features as the measurement of the sea surface complexity.

3.1.1 Majority Intensity Number

The Majority Intensity Number is defined as follow:

$$C_m = Min\left\{\arg\left(\sum_{i=1}^{2^b} X(I)\right) > P_1 N_I\right\} \quad (1)$$

where X is the descending array of the image intensity histogram, 2^b is the number of possible intensity values, P_1 is the percentage which describes the proportion of majority pixels in the image.

3.1.2 Effective Intensity Number

The Effective Intensity Number is defined as follow:

$$C_e = Min\left\{\arg\left(\sum_{i=1}^{2^b} X(I)\right) > (1 - P_2)\, N_I\right\} \quad (2)$$

P_2 is the proportion of random noises in the image and N_I is the number of whole image pixels.

3.1.3 Intensity Discrimination Degree

Although both Majority Intensity Number and Effective Intensity Number can solely help to discriminate different kind of sea surface, using them in combination might result in better intensity discrimination on different sea surfaces.

Intensity Discrimination Degree (IDD) is defined as follows:

$$C_d = \frac{C_m}{C_e} \quad (3)$$

The values of C_d is vary from 0 to 1 which larger indicate more homogenous background sea surface.

3.2 Candidate selection

In this Section, the candidate scoring is introduced. As stated in Section 1.1, sea and inshore ship detection face the same bottleneck: ship extraction from complex backgrounds [16]. By integrating the sea surface analysis, the algorithm used in this thesis could reduce the affecting of the variation of illuminations and sea surface conditions. Second, in the candidate scoring function, the information of both spectral and texture variance is adopted. Combined with the sea-surface-analysis weight, the candidate scoring function is proved to be robust and consistency to variation of sea surfaces, which improve the performance of ship candidate selection in terms of the average recall (AR) [16].

3.2.1 Candidate scoring function

The detector is applied for every location in the input image to find ships regardless its position. Thus, the computational complexity increases drastically. In this stage, we propose the methods which reduce the number of potential-appear ship positions.

Pre-screening of potential ship target is based on the contrast between sea (noise-like background) and target (a cluster of bright/dark pixels) [1]. The intensity abnormality and the texture abnormality suggested in [4] are two key features used for ship segmentation. The 256 x 256 pixels sliding window is applied to the image pixel value to evaluate the abnormality of pixel brightness.

$$d(x,y) = C_d \frac{1}{f(x,y)} + (1 - C_d)\frac{\sigma}{\mu} \tag{7}$$

where $f(x_{i,j})$ is intensity frequency of pixel$x_{i,j}$, C_d is Intensity Discrimination Degree of given sliding window.

Since the size of the ship is usually small in compare to sliding window, the $f(x_{i,j})$ of ship pixels are considered low. Thus, $1/f(x_{i,j})$ is used to emphasize the abnormality of the ship intensity.

The second part of above equation is for texture abnormality. The variance based method using standard deviation σ of a region R centered at the pixel (x, y) is employed to measure the texture roughness of sea surface due to its simplicity and statistical significance. The region size had been chosen empirically of 5 × 5 pixels and is normalized by the mean intensity frequencyμ. Due to the difference of intensities between ships and waters, σ/μ for the edges of the ship is usually high. Thus, it was used to emphasize the texture abnormality at the edges of the ship.

For the homogeneous sea surface, the difference between the intensity values of ship and background is weakened. Hence, higher weight should be set to the texture abnormality in case of smallC_d. In contrary, higher weights should be set to intensity abnormality on sea surfaces with large C_d values, where the intensity abnormality is more effective for ship identification.

3.2.2 Semi-Automatic threshold

In the scene of sea and ships, the pixels of ship as well as other interference object would generate higher $d(x, y)$ values than the sea surface. Therefore, ship candidates can be extracted by finding high peaks of scoring values. It means that the score values of pixels belong to ship or other foreground object should behave as outliers and fall in the right tail of the image distribution. For a given value α, Change et al. [25] define a rejection region denoted by $R(\alpha) = \{r | d(r) < \alpha\}$, by the set made up of al the image pixels in the scoring image whose candidate score values are less than α. The rejection probability $P(\alpha)$ is defined as:

$$P(\alpha) = \Pr(R(\alpha)) \quad (8)$$

The threshold α_0 for detecting anomalies can be determined by setting a confidence coefficient γ such that $P(\alpha) = \gamma$ [Chang and Chiang]. The confidence coefficient γ can be empirically adjusted. When the value of confidence coefficient γ close to 1, only a few targets will be detected as anomalies. This is the case of under segmentation where no pixels are considered as foreground. In contrast, if confidence coefficient γ, most of image pixels would be extracted as anomalies. In this scenario, ship's pixels will be merged with background pixels and destroy its shape information.

3.3 Classification

The goal of this section is to further investigate the extracted ship candidates and to find out the real ships.

3.3.1 Features extraction

a. Features set

According to [1], a ship can be generally described by the following characteristics:

- bright pixels over homogeneous low intensity sea pixels
- known length to width ratio,
- symmetry between its head and tail, like a long narrow ellipse
- a regular and compact shape

In this thesis, several features including shape, texture and spectral based on the ones proposed by [1] are investigated (Table 3.1). In the first category, first order spectral features were considered including mean, standard deviation, min, max and asymmetry coefficient of pixels. Typically, shape features have strong

discriminative powers to describe the shape of the ship target. Moreover, the calculation of these features has a low computing complexity. Concerning texture, first and second order texture measures were derived from either the Grey-Level Co-occurrence Matrix (GLCM). GLCM is a statistical method of examining texture that considers the spatial relationship of pixels. The GLCM functions characterize the texture of an image by calculating how often pairs of pixel with specific values and in a specified spatial relationship occur in an image, creating a GLCM, and then extracting statistical measures from this matrix. Texture properties of GLCM used in this thesis were calculated following [33].

Table 3.1. List of 3 categories features

Group	**Features**	**Description**
Spectral	Number of intensity	The number of intensity values of the component
	Mean	the mean of the intensities of the pixels of the component
	Standard Deviation	the standard deviation of the intensities of the pixels of the component
	Min	the minimum level of any pixel in the component
	Max	the maximum level of any pixel in the component
	Kurtosis	measure of the "tailed-ness" of the probability distribution of intensities values of the component
	Asymmetry	measure of the asymmetry of the probability

	coefficient	distribution of intensities values of the component
Shape	Perimeter	the length of the perimeter of the component
	Area	the area (number of pixels) of the component
	Compactness	the area of the component relative to the perimeter length
	Major axe	the length of the major axis of the ellipse that has the same normalized second central moments as the component
	Minor axe	the length of the minor axis of the ellipse that has the same normalized second central moments as the component
	Ratio Major axe/ Minor axe	the major axe of the component relative to the minor axe
	Extent	the ratio of contour area to bounding rectangle area
	M1	First moment of inertia of the pixels of the component
	M2	Second moment of inertia of the pixels of the component
	M3	Third moment of inertia of the pixels of the component
	M4	Fourth moment of inertia of the pixels of the

		component
Texture	GLCM Dissimilarity	$\sum_{i,j=0}^{N-1} GLCM_{i,j} \times \lvert i-j \rvert$
	GLCM Contrast	$\sum_{i,j=0}^{N-1} GLCM_{i,j} \times (i-j)^2$
	GLCM Homogeneity	$\sum_{i,j=0}^{N-1} \frac{GLCM_{i,j}}{1+(i-j)^2}$
	GLCM Correlation	$\sum_{i,j=0}^{N-1} GLCM_{i,j} \times \left[\frac{(i-\mu_i)(j-\mu_j)}{\sqrt{\sigma_i{}^2 \sigma_j{}^2}}\right]$
	GLCM Energy	$\sqrt[2]{\sum_{i,j=0}^{N-1} GLCM_{i,j}{}^2}$

b. Principle Components Analysis

Ship detection can be considered as n-dimensional classification problem. Such a high dimensional data set requires a large training sample while a limited amount of ground truth information is available concerning ship position. Therefore, Principle Components Analysis (PCA) is used reduce input dimensionality to obtain a classifier that performs well in term of both training and test accuracies.

PCA allows us to find the direction along which data varies the most. The result of running PCA on the set of data called *eigenvectors* which are the *principal components* of the data set. The size of each eigenvector is encoded in the

corresponding eigenvalue and indicates how much the data vary along the principal component. The beginning of the eigenvectors is the center of all points in the data set. Applying PCA to N-dimensional data set yields N N-dimensional eigenvectors, N eigenvalues and 1 N-dimensional center point.

Suppose a random vector population x, where:

$$x = (x_1, x_2, \dots, x_n)^T \tag{9}$$

The mean of that population is denoted by

$$\mu_x = E\{x\} \tag{10}$$

The covariance matrix of the same data set is:

$$C_x = E\{(x - \mu_x)(x - \mu_x)^T\} \tag{11}$$

The components of C_x, denoted by C_{ij}, represent the covariances between the random variable components x_i and x_j. The component C_{ij} is the variance of the component x_i. The variance of a component indicates the spread of the component values around its mean value. If two components x_i and x_j of the data are uncorrelated, their covariance is zero $c_{ij} = c_{ji} = 0$. The covariance matrix is, by definition, always symmetric.

From a sample of vectors $x_1, x_2, \dots, x_M$, the sample mean and the sample covariance matrix can be calculated as the estimates of the mean and the covariance matrix. From a symmetric matrix such as the covariance matrix, we can calculate an orthogonal basis by finding its eigenvalues and eigenvectors. The eigenvectors e_i and the corresponding eigenvalues λ_i are the solutions of the equation:

$$C_x e_i = \lambda_i e_i \; i = 1, \ldots, n \tag{12}$$

For simplicity we assume that the λ_i are distinct. These values can be found, for example, by finding the solutions of the characteristic equation:

$$|C_x - \lambda_i I| = 0 \tag{13}$$

where the I is the identity matrix having the same order than C_x and the $|.|$ denotes the determinant of the matrix. If the data vector has n components, the characteristic equation becomes of order n. This is easy to solve only if n is small. Solving eigenvalues and corresponding eigenvectors is a non-trivial task, and many methods exist. One way to solve the eigenvalue problem is to use a neural solution to the problem. The data is fed as the input, and the network converges to the wanted solution.

By ordering the eigenvectors in the order of descending eigenvalues (largest first), one can create an ordered orthogonal basis with the first eigenvector having the direction of largest variance of the data. In this way, we can find directions in which the data set has the most significant amounts of energy.

Suppose one has a data set of which the sample mean and the covariance matrix have been calculated. Let A be a matrix consisting of eigenvectors of the covariance matrix as the row vectors. By transforming a data vector $\boldsymbol{x}$, we get

$$y = A(x - \mu_x) \tag{14}$$

which is a point in the orthogonal coordinate system defined by the eigenvectors. Components of **y** can be seen as the coordinates in the orthogonal base. We can reconstruct the original data vector x from y by:

$$x = A^T y + \mu_x \tag{15}$$

using the property of an orthogonal matrix $A^{-1} = A^T$. The A^T is the transpose of a matrix . The original vector x was projected on the coordinate axes defined by the orthogonal basis. The original vector was then reconstructed by a linear combination of the orthogonal basis vectors.

Instead of using all the eigenvectors of the covariance matrix, we may represent the data in terms of only a few basis vectors of the orthogonal basis. If we denote the matrix having the K first eigenvectors as rows by A_K , we can create a similar transformation as seen above:

$$y = A_K\ (x - \mu_x) \tag{16}$$

and

$$x = A^T y + \mu_x \tag{17}$$

This means that the original data vector were projected on the coordinate axes having the dimension K and transforming the vector back by a linear combination of the basis vectors. This minimizes the mean-square error between the data and this representation with given number of eigenvectors.

If the data is concentrated in a linear subspace, this provides a way to compress data without losing much information and simplifying the representation. By picking the eigenvectors having the largest eigenvalues we lose as little information as possible in the mean-square sense. One can e.g. choose a fixed number of eigenvectors and their respective eigenvalues and get a consistent representation, or abstraction of the data. This preserves a varying amount of energy of the original data. Alternatively, we can choose approximately the same amount of energy and a varying amount of eigenvectors and their respective eigenvalues. This would in turn give approximately consistent amount of information in the expense of varying representations with regard to the dimension of the subspace.

3.3.2 Classifiers

Finally, three widely used classifiers including Support Vector Machine (SVM), Neural Network (NN) and Decision Tree (DT) are tested in our experiment to find out the best one.

a. Support Vector Machine

A Support Vector Machine (SVM) is a discriminative classifier formally defined by a separating hyper-plane. In other words, given labeled training data (supervised learning), the algorithm outputs an optimal hyper-plane which categorizes new examples.

The operation of the SVM algorithm is based on finding the hyper-plane that gives the largest minimum distance to the training examples. Twice, this distance receives the important name of margin within SVM's theory. Therefore, the optimal separating hyper-plane maximizes the margin of the training data.

A hyper-plane is defined as follow:

$$f(x) = \beta_0 + \beta^T x \tag{18}$$

where β is the weight vector and β_0 is the bias.

The optimal hyper-plane can be represented in an infinite number of different ways by scaling of β and β_0. As a matter of convention, among all the possible representations of the hyper-plane, the one chosen is

$$|\beta_0 + \beta^T x| = 1 \tag{19}$$

where x symbolizes the training examples closest to the hyper-plane. In general, the training examples that are closest to the hyper-plane are called support vectors. This representation is known as the canonical hyper-plane.

the distance between a point x and a hyper-plane (β, β_0) is defined as:

$$d = \frac{|\beta_0 + \beta^T x|}{\|\beta\|} \tag{20}$$

For the canonical hyper-plane, the numerator is equal to one and the distance to the support vectors is

$$d = \frac{|\beta_0 + \beta^T x|}{\|\beta\|} = \frac{1}{\|\beta\|} \tag{21}$$

the margin M is twice the distance to the closest examples:

$$M = \frac{2}{\|\beta\|} \tag{22}$$

The problem of maximizing M is equivalent to the problem of minimizing a function $L(\beta)$ subject to some constraints. The constraints model the requirement for the hyper-plane to classify correctly all the training examples x_i.

$$\min_{\beta\beta_0} L(\beta) = \frac{1}{2}\|\beta\|^2 \text{ subject to } y_i(\beta_0 + \beta^T x_i) \geq 1 \forall i \tag{23}$$

where y_i represents each of the labels of the training examples.

This is a problem of Lagrangian optimization that can be solved using Lagrange multipliers to obtain the weight vector β and the bias β_0 of the optimal hyper-plane.

b. Neural Network

Multilayer Perceptron (ML) implements feed-forward artificial neural networks or, more particularly, multi-layer perceptrons (MLP), the most commonly used type of neural networks. MLP consists of the input layer, output layer, and one

or more hidden layers. Each layer of MLP includes one or more neurons directionally linked with the neurons from the previous and the next layer. Figure 3.2 represents a 3-layer perceptron with three inputs, two outputs, and the hidden layer including five neurons:

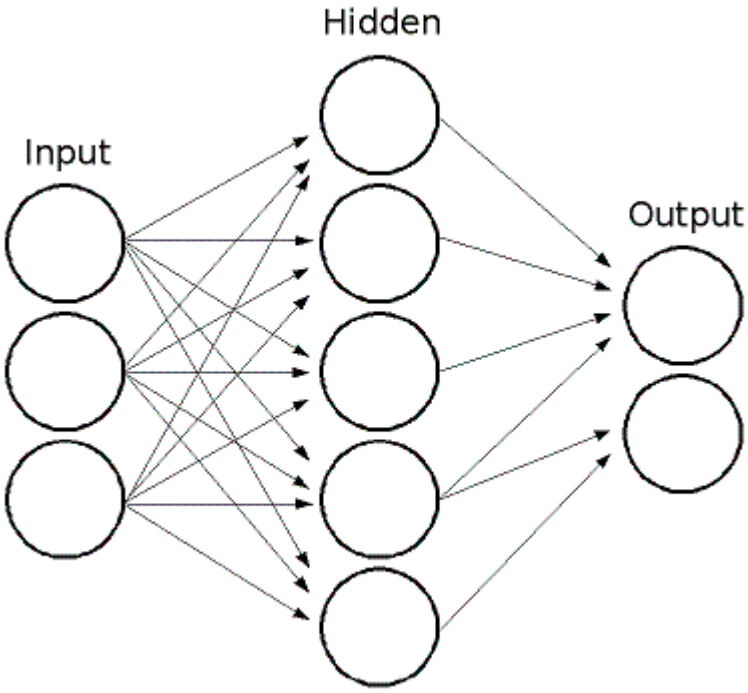

Figure 3.2. Example of MLP

Each of neurons has several input links (it takes the output values from several neurons in the previous layer as input) and several output links (it passes the response to several neurons in the next layer). The values retrieved from the previous layer are summed up with certain weights, individual for each neuron, plus the bias term. The sum is transformed using the activation function f that may be also different for different neurons.

In other words, given the outputs x_j of the layer , the outputs y_j of the layer $n + 1$ are computed as:

$$u_i = \sum_j \left(w_{i,j}^{n+1} \times x_j\right) + w_{i,bias}^{n+1}$$
$$y_i = f(u_i) \tag{24}$$

Different activation functions may be used. Three standard functions are:

Identify function:

$$f(x) = x \tag{25}$$

Sigmoid function:

$$f(x) = \frac{\beta \times (1 - e^{-\alpha x})}{1 + e^{-\alpha x}} \tag{26}$$

Gaussian function:

$$f(x) = \beta \times e^{-\alpha x \times x} \tag{27}$$

c. Decision Tree

A decision tree is a binary tree (tree where each non-leaf node has two child nodes). It can be used either for classification or for regression. For classification, each tree leaf is marked with a class label; multiple leaves may have the same label. For regression, a constant is also assigned to each tree leaf, so the approximation function is piecewise constant.

To reach a leaf node and to obtain a response for the input feature vector, the prediction procedure starts with the root node. From each non-leaf node the procedure goes to the left (selects the left child node as the next observed node) or to the right based on the value of a certain variable whose index is stored in the observed node.

So, in each node, a pair of entities ($variable\_index$, $decision\_rule$ ($threshold/subset$)) is used. This pair is called a split (split on the variable $able\_index$). Once a leaf node is reached, the value assigned to this node is used as the output of the prediction procedure.

Chapter 4 EXPERIMENTS

The whole process of proposed approach is introduced so far. In this Chapter, the dataset and experiment results will be carried out. The proposed method is implemented in Python and Cython for effective parallel processing.

4.1 Datasets

To evaluate the robustness of the ship detection algorithm, we design two datasets of VNREDSat-1 PAN image.

Dataset 1 contains 9 VNREDSat-1 PAN images in the period of 9 months from January 2015 to September 2015 in ocean area. This dataset was used to train and evaluate the performance of the operational method in quite sea conditions. Ships in these images are well discriminated with sea surface. However, an amount percentage of cloud also exists in the scene which may lead to false alarm (Figure 4.1). The full dataset of 9 scenes includes 119 ship objects and 512 non-ship objects. All the images were submitted to the first two processing stages including ship candidate selection and features extraction using PCA provide a training dataset.

Dataset 2 contains 2 VNREDSat-1 PAN images in Saigon Port area. Ships in these images located in Saigon River which show various complex sea-surface textures. The classifier trained by Dataset 1 was used to detect ships in this dataset. This experiment allows exploring the domain of validity and robustness of the proposed operational algorithm. The performance would be quantitatively evaluated.

Images in both datasets are pre-processed to mask out the land area since it’s not in the scope of this thesis.

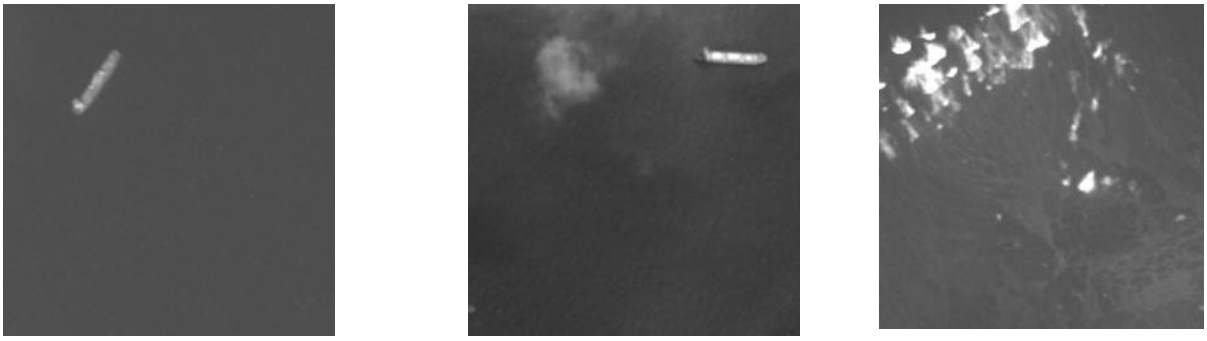

(a) (b) (c)

Figure 4.1. Dataset 1 samples. a) Quite sea b) Cirrus cloud c) Thick cloud. All the images were copped by size 256x256 pixels

Figure 4.2. Dataset 2 samples. All the images were copped by size 256x256 pixels

A dataset of AIS data at the day of images captured in Saigon Port is used as a ground truth of ship's location beside ones located manually. AIS data provide information about latitude and longitude of the ship as well as the timestamp. Location of ships detected in Dataset 2 will be projected into latitude and longitude and compare with AIS data.

4.2 Parameter selection for automatic threshold

Threshold optimization for ship candidate extraction is done using Dataset 1 with ship targets carefully located. The threshold is optimized in order to maximize

the recall of ship targets while minimizing the number of false targets. Besides, the fulfillment of ship target is also considered due to the fact that there are large ships whose body pixels are not homogenous (Figure 4.3). In this thesis, the confidence coefficient γ discussed in Section 3.2.2 is set to the value of 0.9.

Figure 4.3 Heteronomous body ship

In the following experiments, objects segmentation is done using selected threshold. Figure 4.4 shows the binary threshold image on the day of 17th April 2015 using the selected threshold. Figure 4.5 shows the segmented objects including ship and non-ship candidate.

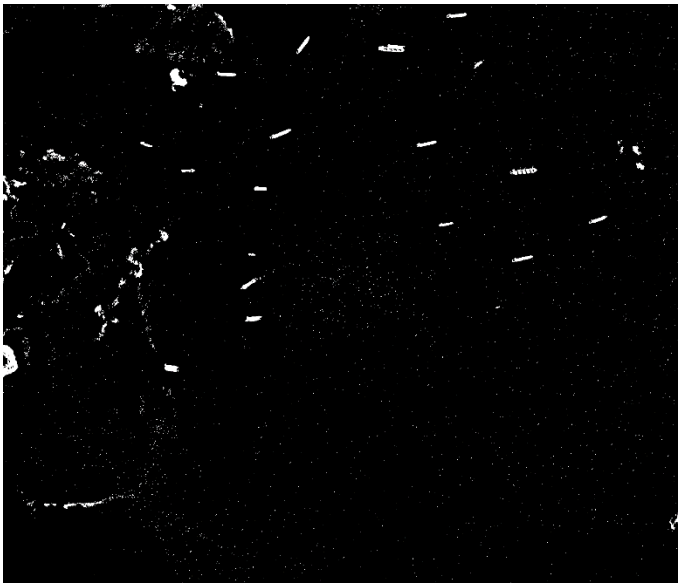

Figure 4.4. Abnormality binary image

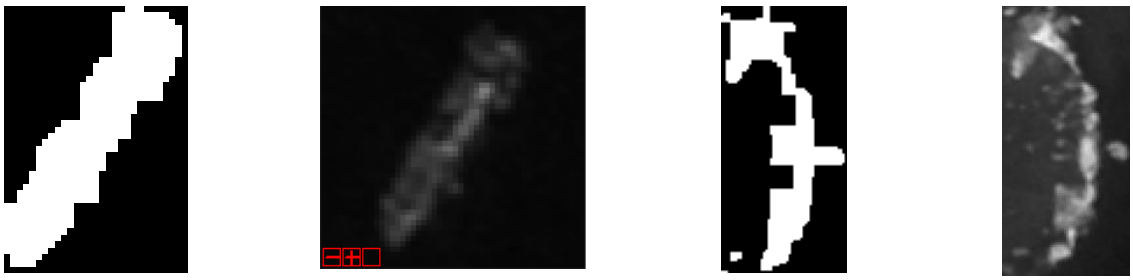

(a) (b) (c) (d)

Figure 4.5. Segmented objects (a) binary mask (b) PAN image of ship target (c) Binary mask and (d) PAN image of non-ship target

4.3 Parameters selection for classifiers

Firstly, Principle Components Analysis (PCA) was used to reduce the size of features space. 8 major components which account to 95% of variance were generated from original 23 features set.

Since well chosen parameters can strongly impact the performance of classifier, parameters that are not directly learnt within estimators can be set by searching a parameter space for the best cross validation score. While grid search is one of the most widely used strategies for parameter optimization, in this article we use random grid search approach which is empirically and theoretically proved to be more efficient [5]. The works were done using python scikit-learn library [6].

Neural Network

The parameters to be optimized are the number of hidden layers, the number of neural nodes and their activation function, learning rate and alpha in each layer and learning rate.

A single hidden layer with sigmoid activation function is proved to be sufficient for most classification task [7][8][9]. Hence, a single hidden layer with sigmoid activation function is used in this work. The $number\ of\ neural\ nodes =$

9 in the hidden layer, $learning\ rate = 0.01$ and $alpha = 0.01$ are found out to give a best score by mean of 10-fold cross-validation using grid-search.

Setting for the random grid search is sampled from the distribution over possible values for each parameter.

SVM

A SVM classifier with RBF kernel is used in this study. Random grid search is performed to find out optimal value of C=1000 and $gamma = 0.0001$ over the possible values.

4.4 Quantitative evaluation

For a detection marked as true positives (*TP*), its referred area S_{inf} coverage must agree with the ground truth object area S_{gt} based in the criterion:

$$\frac{area(S_{inf} \cap S_{gt})}{area(S_{inf} \cup S_{gt})} > 0.8 \tag{28}$$

Each only can match to one; thus, spurious detections of the same object are counted as false positives (FP). Recall and Precision are employed to evaluate the overall performance of proposed ship detection approach. They are defined as:

$$Recall = \frac{Number\ of\ detected\ real\ ship\ targets}{Total\ number\ of\ ship\ targets\ of\ images} \tag{29}$$

$$Precision = \frac{Number\ of\ detected\ real\ ship\ targets}{Number\ of\ detected\ targets} \tag{30}$$

$$F1 - score = 2 \times \frac{Recall \times Precision}{Recall + Precision} \tag{31}$$

4.5 Results and discussion

Table 4.1 shows the average results of 10-folds cross validation for three widely used classifiers including SVM, NN, CART on Dataset 1. Analysis of the results shows that SVM and Neural Network outperform the CART method. Meanwhile, the F-score for SVM and NN respectively 46.15 and 45.86 show insignificance difference of performance. However, SVM is chosen since its precision is much higher than NN (93.2% in compare to 90.2% of NN). Based on experiment results, ship detection classification using SVM seem good enough for near real time application.

Table 4.1. Performance of different classifiers

	Precision (%)	Recall (%)	F1-score
SVM	93.2	92.4	92.3
Neural Network	90.2	93.3	91.72
CART	85.4	68.9	76.26

Addition experiment was done to evaluate the SVM classifier on Dataset 1. Since the same ocean region in different time affected by different weather conditions may results in different sea-surface states, the experiment is carried out as follow. For each image in the dataset as a test image, the rest images of dataset are used as the training data. Performances can be seen in Table 4.2.

Table 4.2. Performance on different sea surface conditions

Test Image Date	**Training set** (#-samples)	**Testing set** (#-samples)	**Precision** (%)	**Recall** (%)
2015/01/17	558	73	91.7	84.6
2015/02/02	540	91	100	100
2015/03/03	567	64	86.7	100
2015/04/17	543	88	100	95.2
2015/05/08	583	48	90.5	90.5
2015/06/09	524	107	100	92.3
2015/07/26	570	61	90	100
2015/08/16	580	51	92.8	86.7
2015/09/04	599	32	100	100

The experiment shows good performance in various scenes. The overall precision and recall of each test is over 90% except for images in 2015/03/03 (precision = 86.7%) and 2015/01/17 (recall = 84.6%) which results still acceptable. Actually, the False Positive in image of 2015/03/03 is just 3 targets. The reduction of precision in image of 2015/03/03 and recall in image of 2015/01/17 are mainly caused by very texture area near the island. Figure 4.6 shows the results where red rectangle locates ships.

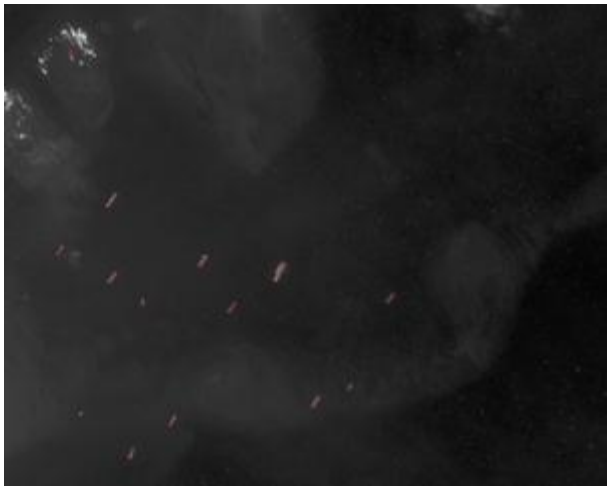

a. 17/01/2015

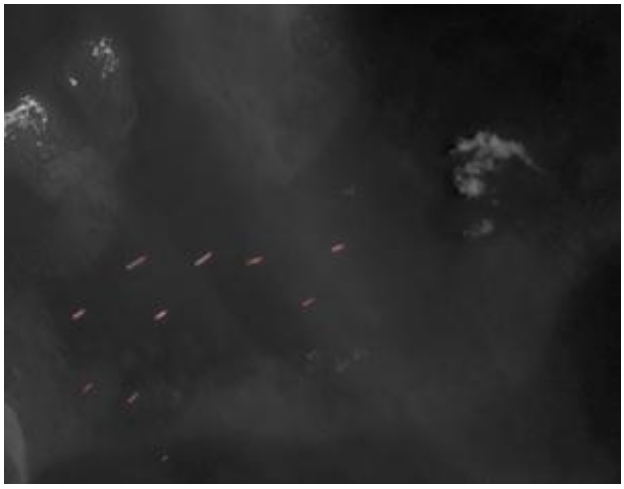

b. 02/02/2015

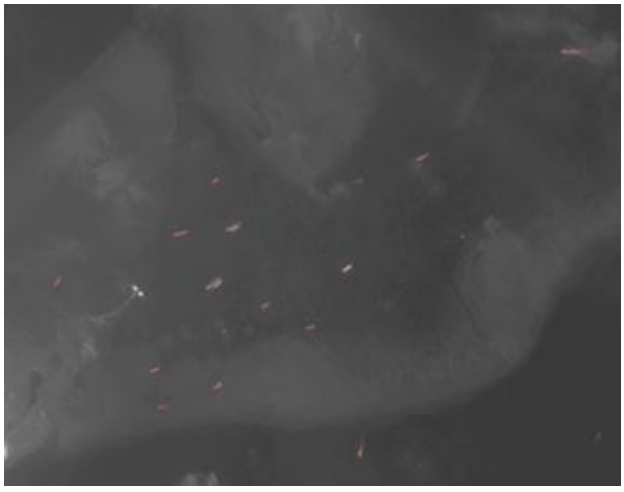

c. 03/03/2015

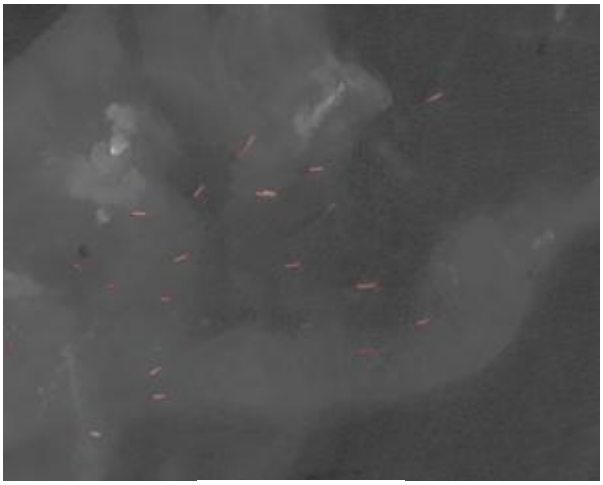

d. 17/04/2015

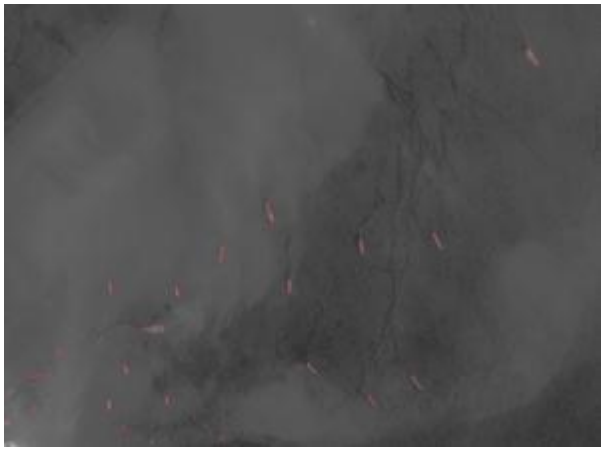

e. 08/05/2015

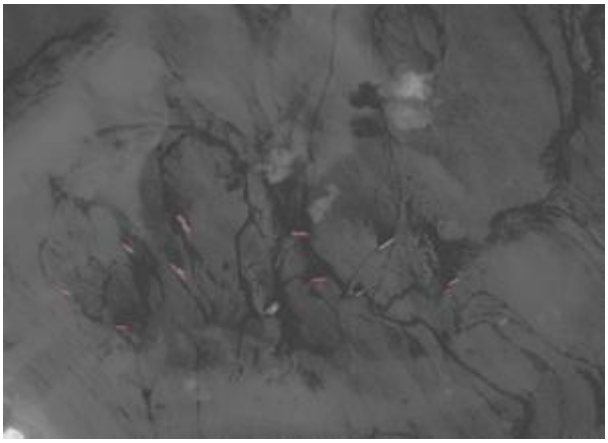

f. 09/06/2015

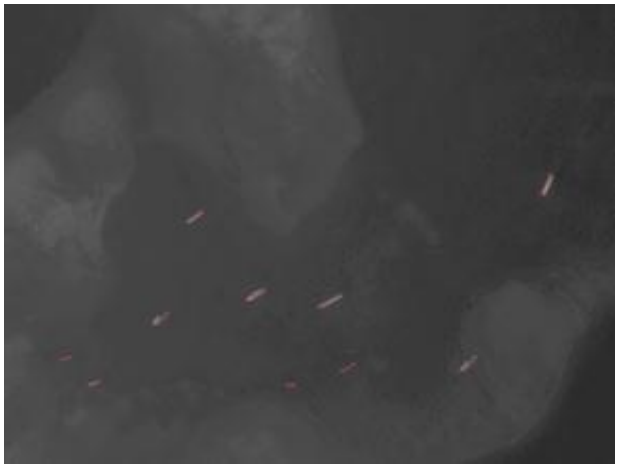

g. 26/07/2015

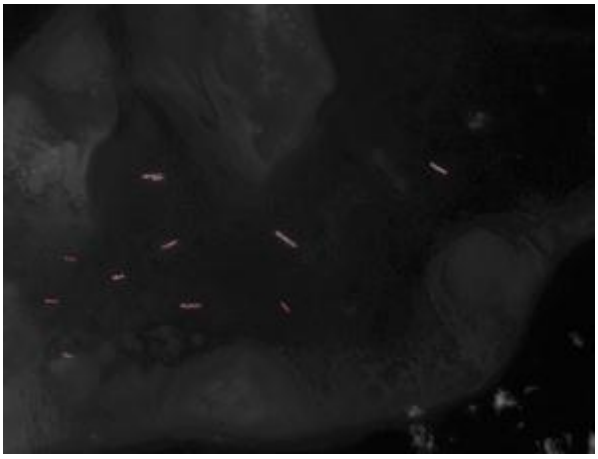

h. 16/08/2015

i. 04/09/2015

Figure 4.6 Results of ship detection in each image scene

Several extreme sea surface conditions strongly impact performance of ship detection procedure. Hence, we evaluate the detection on extreme case of Dataset 2 to demonstrate the robustness of ship detection method which its classifier trained by Dataset 1. Table 4.3 shows the performance of proposed algorithm in Dataset 2. The recall is drastically decreased. This means that proposed method generates false alarms under the interference by texture surface, ship wakes, and etc. Another reason is that proposed method was not design to correctly detect side by side ships. In the case of two or more ships connect side by side, proposed method only

count them as 1. The proposed algorithm proves to be robust in classifying ship targets since the precision does not decrease significantly.

Table 4.3. Operational performance in Dataset 2

Scene date	**Number of ship detected/real ships**	**Recall** (%)	**Precision** (%)	**Matching precision with AIS** (%)
15/04/2015	142/199	71.4	90.4	77.7
28/06/2015	84/107	78.5	92.3	84.6

In order to evaluate the proposed method in real life usage, another metric called “Matching precision with AIS” is used in Table 4.3. This metric describe how the ship’s location detected by satellite image agree with AIS data.

Figure 4.7, Figure 4.8 shows the results where red rectangle locates ships detected by satellite image and green dots are AIS data.

We can see that many ships located by satellite are not reported by AIS data. This phenomenon can be explained by two reasons. First, AIS is not required in port area. Therefore the location of ships reported by AIS is not up-to-date at the time of image captured. Second, since the AIS data is not continuous, the location of ship at the time image captured is the result of an interpolation. This procedure may lead to the large error since the ship trajectory pattern is not simple. This result proves that operational ship detection from satellite image is necessary for management of ship activities.

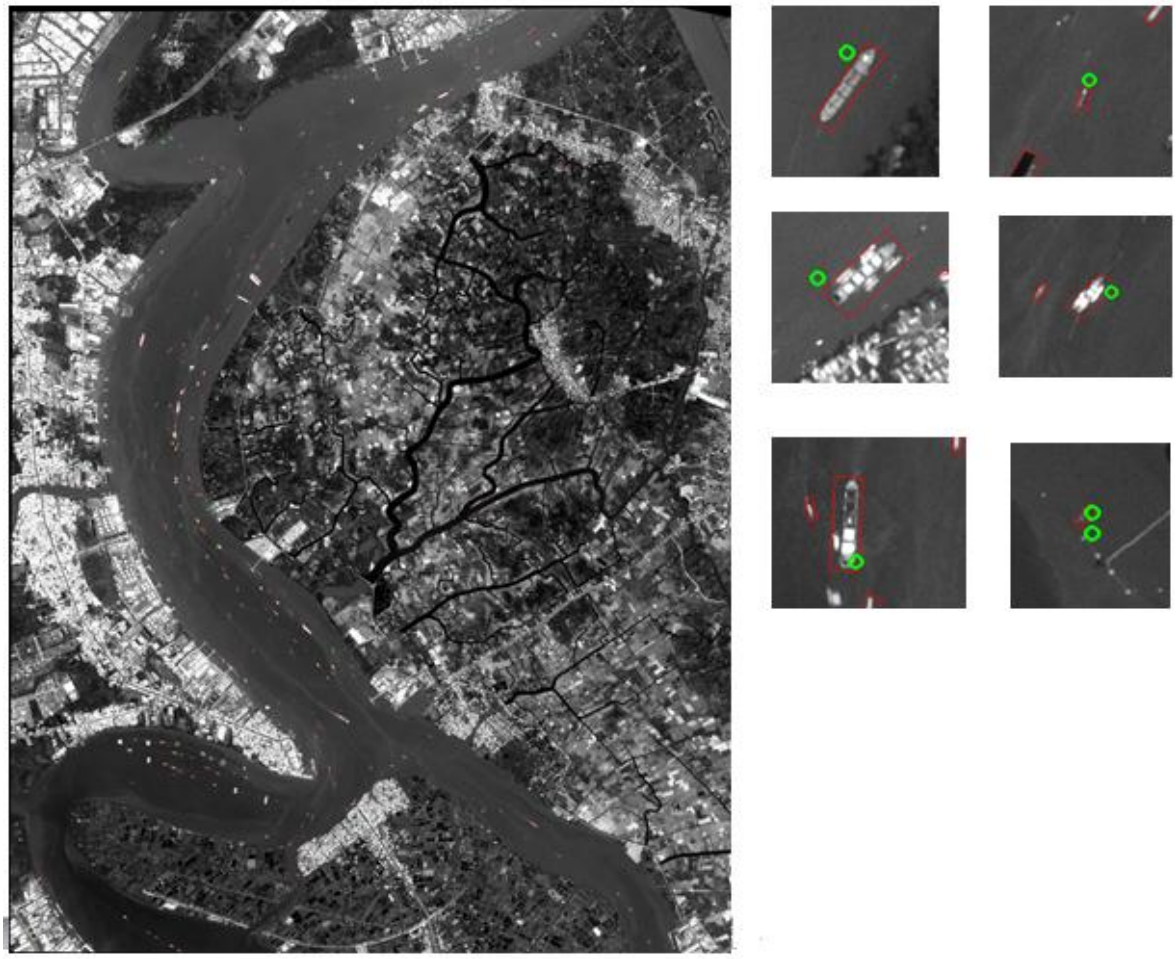

Figure 4.7. Ships detected in Saigon port with AIS data in 15/04/2015

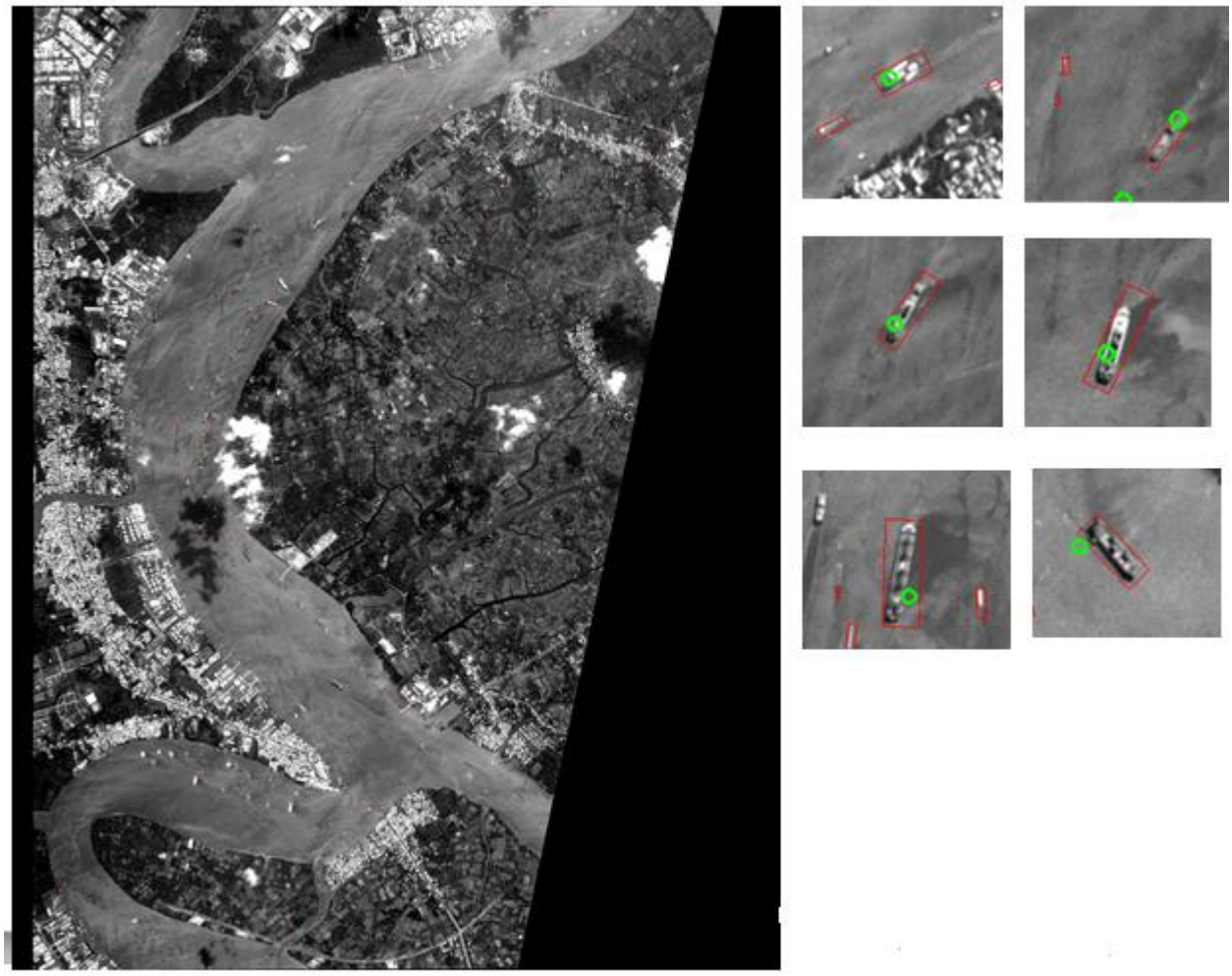

Figure 4.8. Ships detected in Saigon port with AIS data in 28/06/2015

4.6 Web-GIS system

Results of the proposed ship detection framework are successfully deploying to a web-based ship monitoring system for the Vietnam coastal areas. The system can assist in the management maritime of navigation and traffic. It can also be used in case of extreme events or in recuse operations and coastal security. Figure 4.9 shows the Graphical User Interface of the Web-GIS system. The system can be start manually or automatically after new image is inserted into database. Location of ships detected in the image will be displayed as a thematic layer.

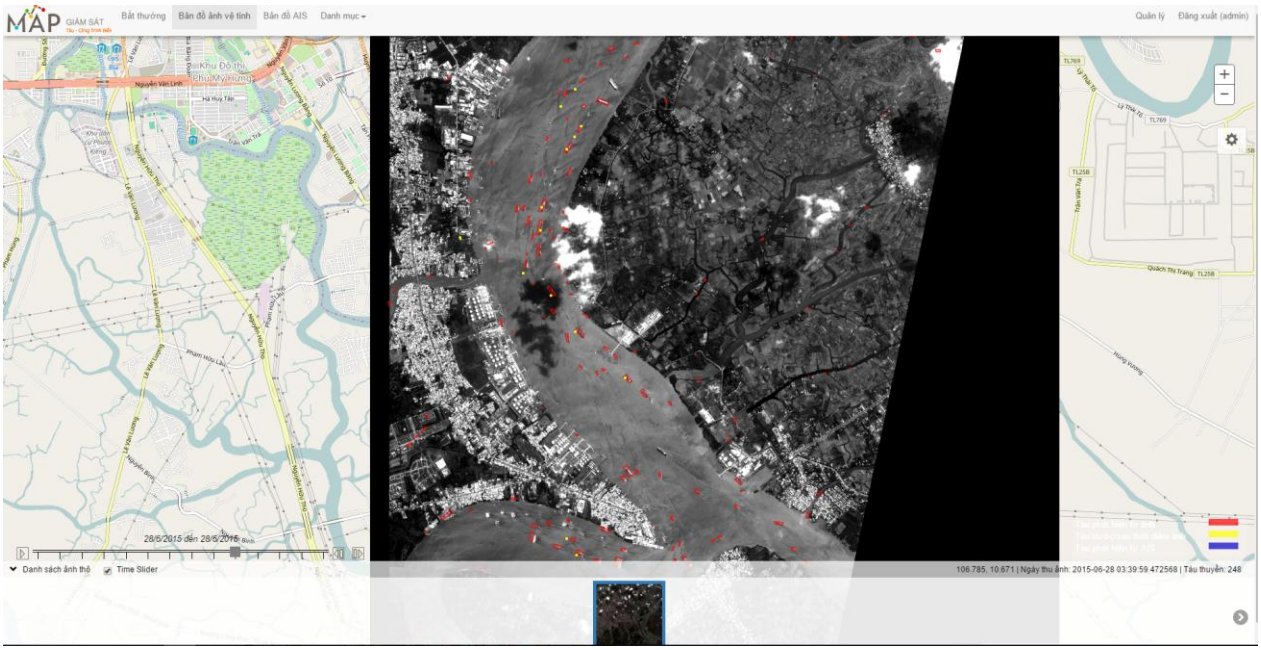

Figure 4.9. Graphical User Interface of the Web-GIS system

To enhance sustainable management in the whole coastal region of Vietnam, there is need to adapt and extent the existing system with other satellite data source to increase both time and location coverage. The proposed ship detection method proved to be robust in different conditions, hence is promising to be applied for other satellite data sources.

Chapter 5 CONCLUSION AND FUTURE WORKS

This thesis analyzes the potential ability of VNREDSat-1 imagery to extract ships on coastal region and proposes an operational ship detection procedure using high-resolution data. What have been done so far in this thesis can be concluded as followed.

First, state-of-the-art report and literature review on ship detection methods using optical satellite image. All methods have been analyzed to point out their advantages and disadvantages and how they can be applied to VNREDSat-1 data.

Second, a complete processing chain for operational ship detection in VNREDSat-1 data is proposed. The sea surface analysis was employed to robustly select the ship candidate objects from image. A semi-automatic threshold is selected to produce a binary image by comparing the abnormality score of foreground objects (ship, wake) with sea as the background. The process can not only inherit the advantages of original method but also make an improvement in term of detection results. Experiment show that the most of the ships are identified correctly regardless of their size, which proves that detecting ships on coastal region using VNREDSat-1 imagery is feasible.

Three lessons learned from this work can be useful for further development of ship detection and management system.

First, aside from the good results achieved, some issues also exist to be further investigated. For example, when dealing with ships near land or low-contrast sea, proposed approach will give poor performance. Further work should focus on these problems to strive for further improvement in this field.

Second, false alarm of the ship detection method can come from the limitation of both radiometric resolution and spatial resolution of image. Low

radiometric resolution decreases discrimination between ship and background. Meanwhile, low spatial resolution make the algorithm hard to classify a candidate target is a ship or not. Further space program development should improve both resolutions.

Last but not least, to surpass the limitation of optical image, an integration system which utilizing SAR image and self-report data such as LRIT, AIS should be considered for more efficient management of ship activities.

REFERENCES

[1] Christina Corbane, Fabrice Marre and Michel Petit, "Using SPOT-5 HRG Data in Panchromatic Mode for Operational Detection of Small Ships in Tropical Area", Sensors, 8, 2959-2973, 2008.

[2] Maider Zamalloa, L.J. Rodríguez-Fuentes, Mikel Peñagarikano, Germán Bordel, and Juan P. Uribe, "Comparing Genetic Algorithms to Principal Component Analysis and Linear Discriminant Analysis in Reducing Feature Dimensionality for Speaker Recognition",GECCO'08, July 12–16, 2008, Atlanta, Georgia, USA

[3] Man Duc Chuc, Kazuki Hao, Bui Quang Hung, Nguyen Thi Nhat Thanh, Yosuke Yamashiki, Dimiter Ialnazov, "Comparision of land cover classifiers for Landsat-8 images a case study in Tien Hai district, Thai Binh province, Red River Delta, Vietnam", "in press"

[4] Guang Yang, Bo Li, Shufan Ji, Feng Gao, and Qizhi Xu ,"Ship Detection From Optical Satellite Images Based on Sea Surface Analysis", IEEE GEOSCIENCE AND REMOTE SENSING LETTERS, VOL. 11, NO. 3, MARCH 2014.

[5] Bergstra, J. and Bengio, Y., "Random search for hyper-parameter optimization", The Journal of Machine Learning Research (2012)

[6] Scikit-learn: Machine Learning in Python, Pedregosa *et al.*, JMLR 12, pp. 2825-2830, 2011.

[7] Zhou L., Yang X., 2008, Use of Neural Networks for Land Cover Classification from Remotely Sensed Imagery. The International

Archives of the Photogrammetry, Remote Sensing and Spatial Information Sciences, Beijing, China, Vol. XXI, Part B7, pp. 575- 578

[8] CYBENKO, G., 1989, Approximation by superpositions of a sigmoidal function. Mathematics of Control, Signals, and Systems, 2, 303–314.

[9] GARSON, G. D., 1998, Neural Networks: An Introductory Guide for Social Scientists (London: Sage).

[10] Tonje N. Hannevik, Øystein Olsen, Andreas N. Skauen and Richard Olsen, "Ship Detection using High Resolution Satellite Imagery and Space-Based AIS"

[11] K. Eldhuset, "An automatic ship and ship wake detection system for space borne SAR images in coastal regions," IEEE Trans. Geosci. Remote Sens., vol. 34, no. 4, pp. 1010–1019, Jul. 1996.

[12] M. V. Dragošvic and P. W. Vachon, "Estimation of ship radial speed ´ by adaptive processing of RADARSAT-1 fine mode data," IEEE Geosci.Remote Sens. Lett., vol. 5, no. 4, pp. 678–682, Oct. 2008

[13] X. Li and J. Chong, "Processing of envisat alternating polarization data for vessel detection," IEEE Geosci. Remote Sens. Lett., vol. 5, no. 2, pp. 271– 275, Apr. 2008.

[14] S. Mirghasemi, H. S. Yazdi, and M. Lotfizad, "A target-based color space for sea target detection," Appl. Intell., vol. 36, no. 4, pp. 960–978, Jun. 2012.

[15] G. Máttyus, "Near real-time automatic marine vessel detection on optical satellite images," Int. Arch. Photogramm. Remote Sens. Spat.

Inf. Sci. – ISPRS Arch., vol. 40, no. 1W1, pp. 233–237, 2013.

[16] Z. Liu, H. Wang, L. Weng, and Y. Yang, “Ship Rotated Bounding Box Space for Ship Extraction from High-Resolution Optical Satellite Images With Complex Backgrounds,” IEEE Geosci. Remote Sens. Lett., vol. 13, no. 8, pp. 1074–1078, Aug. 2016.

[17] C. Grigorescu, N. Petkov, and Michel A. Westenberg, “Contour and boundary detection improved by surround suppression of texture edges,” Image Vis. Comput., vol. 22, no. 8, pp. 609–622, 2004.

[18] C. Grigorescu, N. Petkov, M.A. Westenberg, Contour detection based on nonclassical receptive field inhibition, IEEE Transactions on Image Processing 12 (7) (2003) 729–739.

[19] L. Schwartz. The orie des Distributions. Vol. I, II of Actualite scientifiques et industrielle. L’Institute de Mathematique de l’Universite de Strasbourg, 1950-51.

[20] N. Otsu, “A threshold selection method from gray-level histograms,” IEEE Trans. Syst.,Man, Cybern., vol. SMC-9, no. 1, pp. 62–66, Jan. 1979

[21] C. Zhu, H. Zhou, R. Wang, and J. Guo, “A novel hierarchical method of ship detection from spaceborne optical image based on shape and texture features,” IEEE Trans. Geosci. Remote Sens., vol. 48, no. 9, pp. 3446– 3456, Sep. 2010.

[22] Breiman L, Friedman JH, Olshen RA, Stone CJ. Classification and Regression Trees. CRC Press; 1984

[23] Z. Shi, X. Yu, Z. Jiang, and B. Li, “Ship detection in high-resolution optical imagery based on anomaly detector and local shape feature,” IEEE Trans. Geosci. Remote Sens., vol. 52, no. 8, pp. 4511–4523, 2014.

[24] I. S. Reed and X.Yu, “Adaptive multiple-band CFARdetection of an optical pattern with unknown spectral distribution,” IEEE Trans. Acoust., Speech, Signal Processing, vol. 38, pp. 1760–1770, Oct. 1990.

[25] Chein-I Chang and Shao-Shan Chiang, “Anomaly detection and classification for hyperspectral imagery,” IEEE Trans. Geosci. Remote Sens., vol. 40, no. 6, pp. 1314–1325, Jun. 2002.

[26] G. Cheng et al., “Object detection in remote sensing imagery using a discriminatively trained mixture model,” ISPRS J. Photogramm. Remote Sens., vol. 85, pp. 32–43, Nov. 2013

[27] J. Han, D. Zhang, G. Cheng, L. Guo, and J. Ren, “Object detection in optical remote sensing images based on weakly supervised learning and high-level feature learning,” IEEE Trans. Geosci. Remote Sens., vol. 53, no. 6, pp. 3325–3337, Jun. 2015.

[28] G. Liu et al., “A new method on inshore ship detection in high-resolution satellite images using shape and context information,” IEEE Geosci. Remote Sens. Lett., vol. 11, no. 3, pp. 617–621, Mar. 2014

[29] R. Zhang, J. Yao, K. Zhang, C. Feng, and J. Zhang, “S-CNN-BASED SHIP DETECTION FROM HIGH-RESOLUTION REMOTE SENSING IMAGES,” ISPRS - Int. Arch. Photogramm. Remote Sens.

Spat. Inf. Sci., vol. XLI-B7, pp. 423–430, Jun. 2016.

[30] M. Cheng, Z. Zhang, W. Lin, and P. Torr, “BING: Binarized normed gradients for objectness estimation at 300 fps,” in Proc. IEEE Int. Conf. Comput. Vis. Pattern Recog., 2014, pp. 3286–3293

[31] Z. Zou and Z. Shi, “Ship Detection in Spaceborne Optical Image With SVD Networks,” *IEEE Trans. Geosci. Remote Sens.*, vol. 54, no. 10, pp. 5832–5845, Oct. 2016.

[32] Tran Manh Tuan, “SPACE TECHNOLOGY IN VIETNAM: 2008 COUNTRY REPORT”, APRSAF-15: Space for Sustainable Development, Vietnam December 9-12,2008

[33] The GLCM Tutorial Home Page, http://www.fp.ucalgary.ca/mhallbey/tutorial.htm